JKAU: Eng. Sci., **vol. 11 no. 1,** pp. 211-226 (1419 A.H. / 1999 A.D.)

Performance Analysis of Partially-wet Rectangular Fin Assembly

M.M. SALAH EL-DIN
Mechanical Engineering Department, College of Engineering and Islamic Architecture, Umm Al-Qura University, Makkah, Saudi Arabia

ABSTRACT. Analytical solutions for the performance of the fully-and partially-wet fin assembly has been provided. An assumption that the humidity ratio of the saturated air on the wet surface varies linearly with the local fin temperature was used. The effects of the various parameters including the cold fluid temperature, the air temperature and relative humidity and the fin thermal conductivity on the fin assembly performance and on the temperature distribution have been investigated. Also, the effect of the fin assembly dimensions has been studied. Besides, the model presented is useful in prediction of the wet and dry parts of the fin assembly. Finally, the effect of the fin tip boundary condition has been studied.

Introduction

Finned tube heat exchangers are widely used in applications for air cooling. When the fin surface temperature is below the dew point temperature of the air being cooled, dehumidification of the air occurs. With dehumidification, fin surface is wetted and simultaneous heat and mass transfer exists. Therefore, the study of the performance of the wet-surface heat exchangers is considerably different from the study of dry-surface heat exchangers.

An earlier expression for the efficiency of a wet fin has been developed by Threlkeld [1]. He used the enthalphy difference as the driving force for the combined heat and mass transfer under the assumption that the Lewis number is equal to one. He also assumed a linear relation between the enthalphy and the temperature of the saturated moist air. McQuiston[2] used the difference in the humidity ratio between the incoming air and that existing on the fin surface as the driving force for the mass transfer. He assumed that this difference is linearly related to the corresponding temperature difference.

Coney *et al.*[3] analyzed theoretically the performance of a cooling and dehumidifying vertical rectangular fin. They incorporated the condensate thermal resistance into the analysis and solved the resulting equations numerically. They also presented an experimental investigation of the performance of a vertical rectangular fin when humidification occurs in turbulent flow[4]. The condensation on a vertical plate fin of variable thickness has been studied numerically by Sarma *et al.*[5]. Kazeminejad *et al.*[6] presented a numerical analysis of the performance of a cooling and dehumidifying vertical rectangular fin with non-uniform heat transfer coefficient. Chen *et al.*[7] studied numerically the laminar boundary layer analysis of film condensation on a vertical plate fin in the presence of the interfacial sheat at the condensate-vapor interface.

Wu and Bond[8] provided analytical solutions for the efficiency of a straight fin under both fully wet and partially wet conditions by using the temperature and humidity ratio differences as the driving forces for heat and mass transfer. They assumed a linear relation between the humidity ratio of the saturated air on the wet surface and the local fin temperature.

Recently, Kazeminejad[9] analyzed numerically the performance of a cooling and dehumidifying fin assembly. He assumed that the fins are fully wetted, i.e. the wall and the fin surface temperatures are below the dew point temperature of the surrounding humid air. Although, the results presented showed that the fin surface temperature becomes greater than the dew point temperature of the air after a certain distance from the fin base. This means that after this distance the fin surface is dry and the assumption of fully wet surfaces is not achieved. Therefore, it is better to analyze the problem under the partially wet condition which is more general than the fully wet condition.

In this work, analytical solution for the performance of partially-wet fin assembly has been provided. The model presented is useful in prediction of the wet and dry parts of the fin assembly beside the effect of the various parameters, including the assembly dimensions on the thermal performance.

Analysis

The fin assembly configuration is shown in Fig. 1. Equally spaced rectangular fins are attached to a plane wall. The heat flow within the wall and the fin is assumed to be one dimensional in the x-direction and the thermal contact resistance between them is negligible. Constant thermal conductivities of the wall and the fins are considered and the coefficient of heat transfer over the fin side is assumed to be constant. When the temperatures over the entire surface of the wall and the fin are higher than the dew point of the air, then the surface is fully dry and no condensation occurs. An analytical solution to this case is presented in ref. [9]. If the wall surface temperature is below the dew point of the air but the fin tip temperature is higher, condensation occurs only on a part of the fin, i.e. the fin is partially wetted. In Fig. 1 the length l_0 represents the wet part of the fin. Because of the geometrical and thermal symmetry, it is sufficient to examine the heat flow within regions A, B and C shown in Fig. 1. The dimensionless governing equations for these regions are:

i. Region A

$$\frac{d^2\theta_w}{dX^2} = 0$$

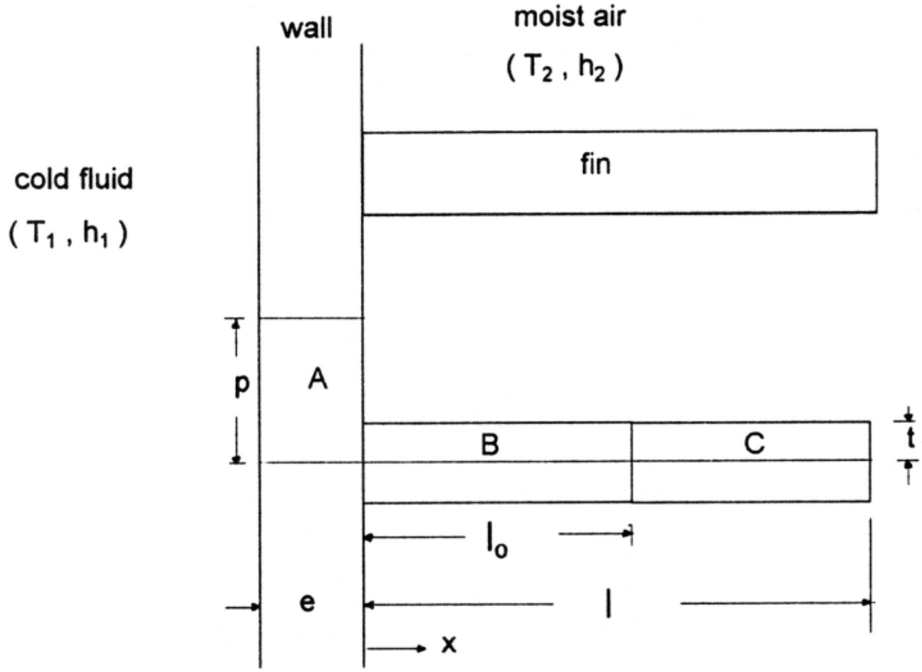

(1)

FIG. 1. Configuration of the partially wet fin assembly.

The boundary conditions are

$$\text{at } X = -E: \quad \frac{d\theta_w}{dX} = -Bi_1(1-\theta_w) \tag{2}$$

$$\text{at } X = 0: \quad \frac{d\theta_w}{dX} = KP\frac{d\theta_f}{dX} - Bi_2(1-P)\left(\theta_b + h_{fg}\frac{K_m}{h_2}\cdot\frac{W_b - W_2}{T_1 - T_2}\right) \tag{3}$$

The coefficients of heat and mass transfer are related by the Chilton and Colburn analogy[10]:

$$\frac{h_2}{K_m} = c_p Le^{2/3} \tag{4}$$

Substitution in Eq. (3) gives

$$\left.\frac{d\theta_w}{dX}\right|_{X=0} = KP\left.\frac{d\theta_f}{dX}\right|_{X=0} - Bi_2(1-P)\left(\theta_b + \zeta\frac{W_b - W_2}{T_1 - T_2}\right) \tag{5}$$

$$\zeta = \frac{h_{fg}}{c_p Le^{2/3}}$$

where

ii. Region B

$$\frac{d^2\theta_f}{dX^2} - m_o^2(\theta_f + \zeta \frac{W_f - W_2}{T_1 - T_2}) = 0 \qquad (6)$$

$$m_0^2 = Bi_2 / KP$$

where

The boundary conditions are

at $X = 0$, $\theta_f = \theta_b$ (7)

at $X = L_0$, $\theta_f = \theta_d$ (8)

iii. Region C

$$\frac{d^2\theta_f}{dX^2} - m_o^2\theta_f = 0 \qquad (9)$$

The boundary conditions are

at $X = L_0$, $\theta_f = \theta_2$ (10)

at $X = L$, $\frac{d\theta_f}{dX} = -\frac{Bi_2}{K}\theta$ (11)

The solution to Eq. (9) with the described boundary conditions gives the temperature distribution of the dry part of the fin

$$\frac{\theta_f}{\theta_d} = \frac{\cosh[m_0(L-X)] + \sqrt{\frac{Bi_2P}{K}}\sinh[m_0(L-X)]}{\cosh[m_0(L-L_0)] + \sqrt{\frac{Bi_2P}{K}}\sinh[m_0(L-L_0)]} \qquad (12)$$

To solve Eq. (6) the relation between W_f and T_f is required. Wu and Bong[8] assumed a linear relation

$$W_f = a + bT_f \qquad (13)$$

where

$$a = W_b - \frac{W_0 - W_b}{T_0 - T_b} T_b \qquad (14)$$

and

$$b = \frac{W_0 - W_b}{T_0 - T_b} \qquad (15)$$

Substituting Eq. (13) into Eq. (6) and rearranging

$$\frac{d^2\theta_f}{dX^2} - m_0^2(1 + b\zeta\cdot)\theta_f - m_0^2\zeta \cdot C_o = 0 \qquad (16)$$

where

$$C_o = \frac{a + bT_2 - W_2}{T_1 - T_2}$$

The solution to Eqs. (16), (7) and (8) gives the temperature distribution of the wet part of the fin

$$\frac{\theta_f + \theta_p}{\theta_b + \theta_p} = \frac{\dfrac{\theta_d + \theta_p}{\theta_b + \theta_p} \sinh(mX) + \sinh[m(L_0 - X)]}{\sinh(mL_0)} \tag{17}$$

where

$$\theta_p = \frac{\zeta \cdot C_o}{1 + b\zeta} \qquad \text{and} \qquad m^2 = m_0^2(1 + b\zeta \cdot)$$

Using Eq. (13) and Eq. (17) with Eqs. (1), (2) and (5) gives the temperature distribution within the wall

$$\theta_w = 1 + \frac{KPm[(\theta_d + \theta_p)\mathrm{cosech}(mL_0) - (1 + \theta_p)\coth(mL_0)] - Bi_2(1-P)[1 + \zeta\cdot(C_o + b\theta_b)]}{1 + (E + \dfrac{1}{Bi_1})[KPm \cdot \coth(mL_0) + Bi_2(1-P)]} * (X + E + \frac{1}{Bi_1}) \tag{18}$$

From Eqs. (12), (17), and (18) it is clear that the temperature distribution can be determined if L_0 and θ_b are known. The continuity of heat flow at the point separating the wet and dry surfaces, i.e. at $X = L_0$ gives

$$\left.\frac{d\theta_f}{dX}\right|_{X=L_0^-} = \left.\frac{d\theta_f}{dx}\right|_{X=L_0^+} \tag{19}$$

Differentiation of Eqs. (12) and (17) and substitution into Eq. (19) gives

$$\frac{m}{\sinh(mL_0)}\left[(\theta_d + \theta_p)\cosh(mL_0) - (\theta_b + \theta_p)\right]$$

$$= \frac{-m_o\theta_d\left\{\sinh[m_o(L - L_0)] + \sqrt{\dfrac{Bi_2P}{K}}\cosh[m_o(L - L_0)]\right\}}{\cosh[m_o(L - L_0)] + \sqrt{\dfrac{Bi_2P}{K}}\sinh[m_o(L - L_0)]} \tag{20}$$

By using the iterative procedure shown in the appendix, L_0 and θ_b can be determined.

Effectiveness of the fin assembly

Effectiveness is defined as the ratio of the heat transfer rate of the finned assembly to that of the unfinned wall at the same conditions. Mathematically, effectiveness is expressed as

$$\varepsilon = \left[\left(\frac{d\theta_w}{dX} \right) / \left(\frac{d\theta_w^*}{dX} \right) \right]_{X=0} \tag{21}$$

In order to evaluate the effectiveness of the fin assembly, the solution of the energy equation within the unfinned wall is first required. It is

$$\frac{d^2\theta_w^*}{dX^2} = 0 \tag{22}$$

The boundary conditions are

$$\text{at } X = -E \quad , \quad \frac{d\theta_w^*}{dX} = -Bi_i(1 - \theta_w^*) \tag{23}$$

$$\text{at } X = 0 \quad , \quad \frac{d\theta_w^*}{dW} = -Bi_2\theta_w^* - Bi_2\zeta \cdot (C_o + b\theta_w^*) \tag{24}$$

The solution to the above equations give the temperature distribution within the unfinned wall:

$$\theta_w^* = \frac{-Bi_2[1 + \zeta \cdot (C_o + b\theta_w^* \big|_{x=0})]}{1 + Bi_2(E + \dfrac{1}{Bi_1}} (X + E + \frac{1}{Bi_1}) + 1 \tag{25}$$

Differentiating Eq. (17) and substituting into Eq. (5) gives $d\theta_w / d\theta_w / dX\big|_{x=0}$ and substituting Eq. (25) into Eq. (24) gives $D\theta_w^* / dX\big|_{x=0}$. So, the effectiveness can be obtained from Eq. (21)

Insulated fin tip

For insulated fin tip the boundary conditions of region C are

$$\text{at} \quad X = L_0 \quad , \quad \theta_f = \theta_d \tag{26}$$

$$\text{at} \quad X = L \quad , \quad d\theta_f / dX = 0 \tag{27}$$

The solution to Eq. (9) at the above boundary conditions gives the temperature distribution of the dry part of the fin

$$\frac{\theta_f}{\theta_d} = \frac{\cosh[m_o(L - X)]}{\cosh[m_o(L - L_0)]} \tag{28}$$

The length of the wetted part of the fin can be determined using the condition given by Eq. (19)

$$\frac{m}{\sinh(mL_0)}[(\theta_d + \theta_p)\cosh(mL_0) - (\theta_b + \theta_p)]$$

$$= -m_o\theta_d \tanh[m_o(L - L_0)] \tag{29}$$

By using the iterative procedure in the appendix, L_0 and θ_b can be determined. Consequently, the effectiveness of the fin assembly can be attained as explained before.

Fully-wet fin assembly

When the fin tip temperature is equal to or below the dew point of the air, the fin assembly will be fully wetted. Following the previous procedure, but for two regions only, the temperature distribution can be obtained.

Within the fin, the temperature distribution is given by

$$\theta_f + \theta_p = [(\theta_b + \theta_p)\cosh[m(L - X)] - \frac{Bi_2}{mK}[\theta_t + \zeta(C_o + b\theta_t)]\sinh(mX)] \\ / \cosh(mL) \tag{30}$$

and within the wall the temperature distribution is given by

$$\theta_w = \frac{-KPm(1+\theta_p)\tanh(mL) - \dfrac{Bi_2 P}{\cosh(mL)}[\theta_t + \zeta(C_o + b\theta_t)] - Bi_2(1-P)[1+\zeta(C_o + b\theta_w)]}{1 + (\dfrac{1}{Bi_1} + E)[Bi_2(1+P) + KPm\cdot\tanh(mL)]} \\ *(X + E + \frac{1}{Bi_1}) + 1 \tag{31}$$

From Eqs. (30) and (31) it is clear that to obtain the effectiveness of the fin assembly the fin tip temperature must be known. One may say that the fin tip temperature is equal to the dew point of the air, but what make us sure that for a specified fin assembly, through which the air flows at a known condition, the fin tip temperature will be equal to the dew point of the air? As will be seen later, it is generally not possible to achieve the complete wetness of the fin except for few cases.

Results and Discussion

The procedure described in the appendix has been used to calculate the temperature distribution, the length of the wetted part of the fin and the effectiveness of the fin assembly. Usually, the relative humidity of the air is used instead of the humidity ratio which appeared in the analysis. Therefore, it will be used here with the relations in ref. [10].

Fig. 2 illustrates the location separating the wet and dry parts of the fin as a function of the relative humidity of the air for different lengths of the fin. From the figure it is clear that the wet region increases with the increase of the air relative humidity. The ratio of the wet length of the total length of the fin decreases with the increase of the fin length at the same relative humidity. Also, the effect of the air relative humidity decreases with the increase of the fin length. For long fins it is not possible to get fully wet surfaces at the given conditions.

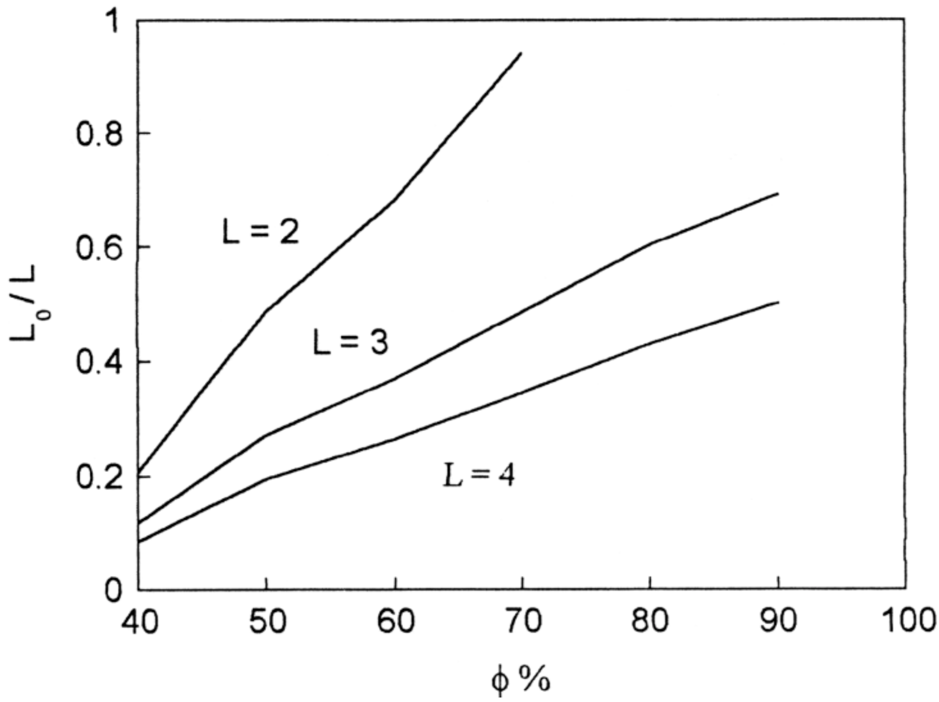

FIG. 2. The location separating the wet and dry parts of the fin ($K = 1$, $Bi_1 = 1$, $Bi_2 = 0.1$, $P = 0.25$, $E = 0.5$, $T_1 = 0°C$, $T_2 = 25°C$).

The temperature distribution within the wall and the fin is given in Fig. 3 for different air relative humidities. The figure shows that θ decreases as relative humidity is increased. The increase in the relative humidity results in higher condensation on the fin surface and hence higher latent heat transfer and higher fin surface temperature. This explains the increase in the wet region with the increasing in the air relative humidity.

The variation of the effectiveness with the fin length and the air relative humidity is shown in Fig. 4. The effectiveness approaches a limiting value as the fin length increases. This can be explained by the fact that the fins, which increase the heat transfer area, introduce conductive resistance to the heat flow. First, the increase in the surface area is more effective than the conductive resistance, but further increase in the fin length gets a state that the two have the same effect. Mathematically, the temperature gradient $(d\theta_w/dX)|_{X=0}$ becomes approximately constant for large values of L [see Eq. (18)]. Fig. 4 shows also that the effectiveness increases with the decrease in the air relative humidity. The effectiveness reaches its maximum value when dry air ($\phi = 0$) is flowing over the fins. At this special case the fins are fully dry and the effectiveness is calculated from the following relation[9]

$$\varepsilon = \frac{\dfrac{1}{Bi_1} + E + \dfrac{1}{Bi_2}}{\dfrac{1}{Bi_1} + E + \dfrac{\zeta}{Bi_2}} \tag{32}$$

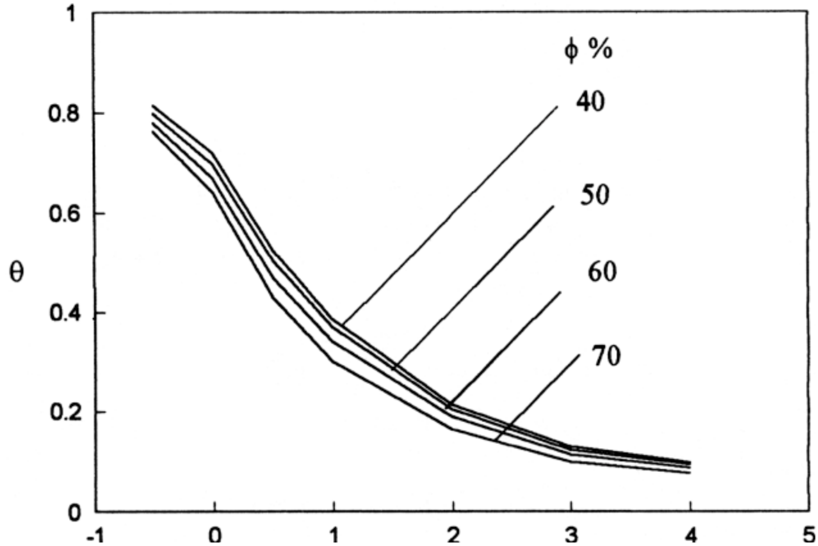

FIG. 3. The location distribution within the wall and the fin (K = 1, Bi_1 = 1, Bi_2 = 0.1, P = 0.25, E = 0.5, L = 4, T_1 = 0ºC, T_2 = 25ºC).

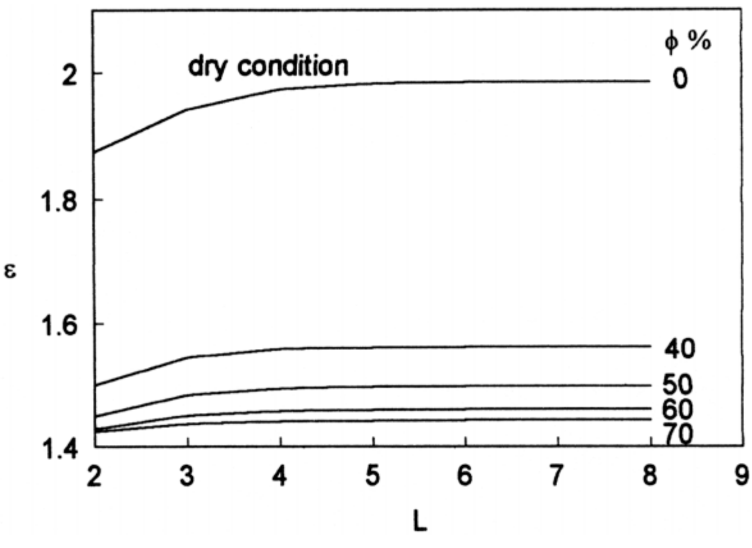

FIG. 4. The variation of the effectiveness with the fin length and the air relative humidity (K = 1, Bi_1 = 1, Bi_2 = 0.1, P = 0.25, E = 0.5, T_1 = 0ºC, T_2 = 25ºC).

where

$$\xi = \frac{Bi_2}{Bi_2(1-P) + K\sqrt{Bi}\left[\dfrac{\sinh(\frac{L}{P}\sqrt{Bi}) + \sqrt{Bi}\cdot\cosh(\frac{L}{P}\sqrt{Bi}}{\cosh(\frac{L}{P}\sqrt{Bi}) + \sqrt{Bi}\cdot\sinh(\frac{L}{P}\sqrt{Bi}}\right]} \tag{33}$$

and

$$Bi = Bi_2 P / K \tag{34}$$

The effect of cold fluid temperature is shown in Fig. 5. The increase in T_1 increases the fin surface temperature and hence the dry part of the fins and the effectiveness increase. Conversely, the increase in T_2 increases the wet part of the fins slightly and hence a slight decrease in the effectiveness is obtained as shown in Fig. 6.

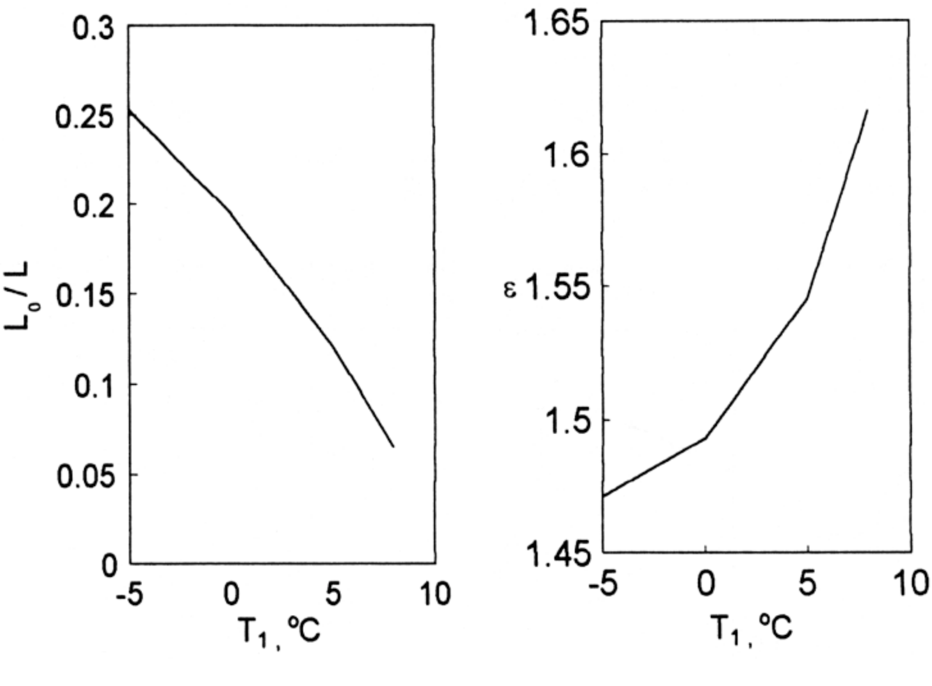

FIG. 5. The effect of the cold fluid temperature (K = 1, Bi_1 = 1, Bi_2 = 0.1, P = 0.25, E = 0.5, ϕ = 50%, L = 4, T_2 = 25ºC).

Fig. 7 shows the effect of the fin thermal conductivity compared to the wall thermal conductivity on ε and L_0/L. The rate of heat transfer within the fins increases with higher thermal conductivities and hence both the effectiveness and the wet region increase. Increasing the fin thickness compared to the fin pitch leads also to the increase in the effectiveness and the wet region as shown in Fig. 8. The increase in the effectiveness due to the increase in P is smaller than that due to the increase in K and approaches a limiting value. This may be explained by the increase in the fin thermal conductive resistance with the increase in its cross-sectional area.

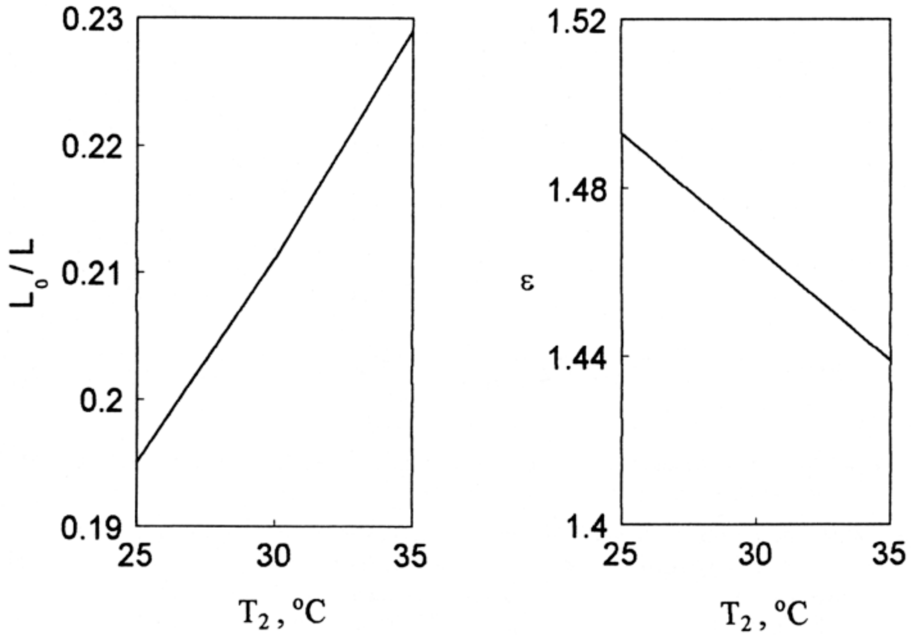

FIG. 6. The effect of the air temperature (K = 1, Bi_1 = 1, Bi_2 = 0.1, P = 0.25, E = 0.5, T_1 = 0ºC, ϕ = 50%, L = 4).

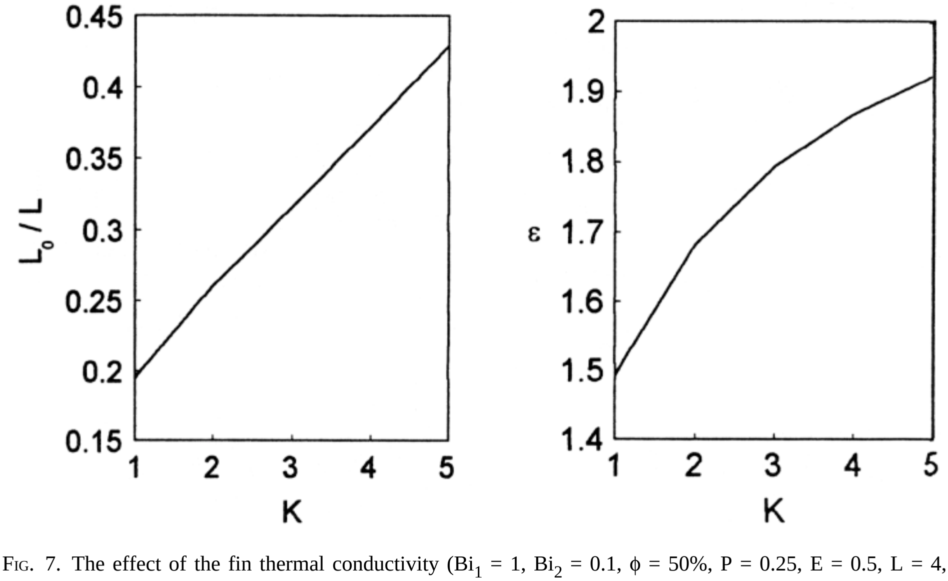

FIG. 7. The effect of the fin thermal conductivity (Bi_1 = 1, Bi_2 = 0.1, ϕ = 50%, P = 0.25, E = 0.5, L = 4, T_1 = 0ºC, T_2 = 25ºC).

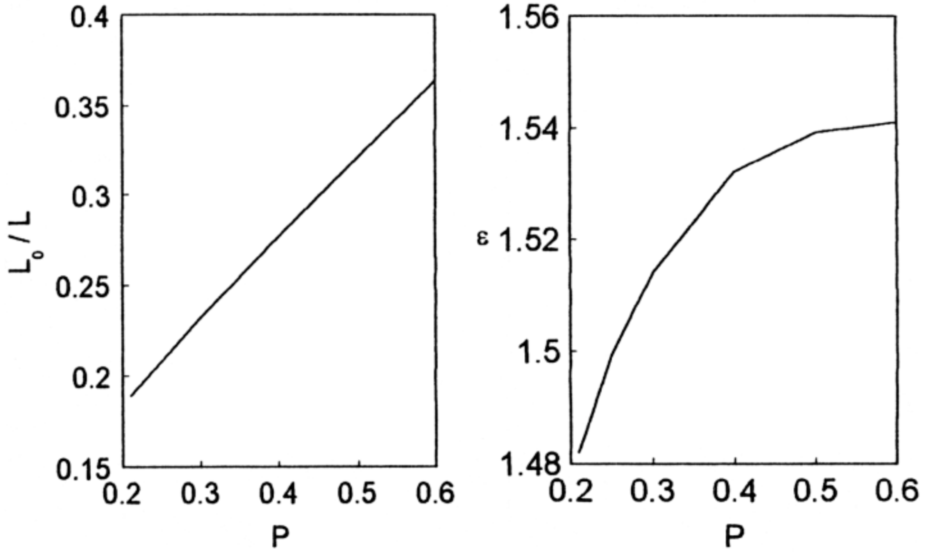

FIG. 8. The effect of the fin thickness (K = 1, Bi_1 = 1, Bi_2 = 0.1, E = 0.5, L = 2, ϕ = 40%, T_1 = 0ºC, T_2 = 25ºC).

When the fin tip is insulated the rate of heat transfer within the fin is decreased and hence the effectiveness is decreased. This effect vanishes as the fin length increases and the effectiveness becomes as same as for the uninsulated fin tip as shown in Fig. 9. From the figure it can also be seen that the difference in the wet region vanishes with the increase in the fin length.

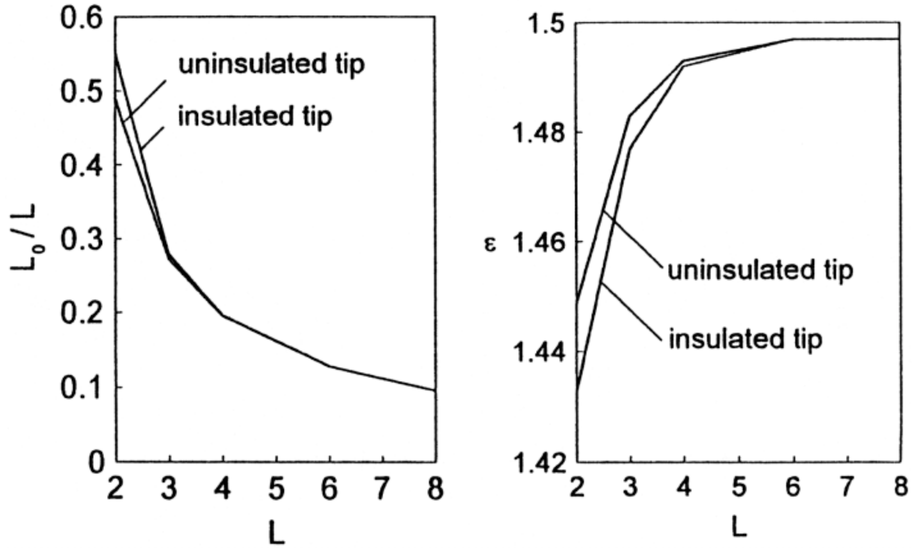

FIG. 9. The effect of the fin tip boundary condition (K = 1, Bi_1 = 1, Bi_2 = 0.1, P = 0.25, E = 0.5, ϕ = 50%, T_1 = 0ºC, T_2 = 25ºC).

Conclusions

The performance of the partially-wet fin assembly has been studied and analytical solutions have been obtained when the fin assembly operates under fully wet and partially wet conditions. From the results it can be concluded that :

1 – The fully-wet condition can be achieved for shorter fins and higher air relative humidity. When the fins become longer, partially-wet condition exists.

2 – The increasing in the air relative humidity increases the fin surface temperature but decreases the fin effectiveness.

3 – The effectiveness of the fin assembly increases with the increase of the cold fluid temperature, the fin thermal conductivity and the fin dimensionless thickness. Conversely, the increasing in the air temperature decreases slightly the effectiveness.

4 – The effectiveness approaches a limiting value as the fin length increases.

5 – The ratio L_0/L increases with the increase in the air temperature, the fin thermal conductivity and the fin dimensionless thickness. The ratio decreases with the increase in the cold fluid temperature and the fin length.

6 – When the fin tip is insulated a small decrease in the effectiveness and a small increase in the ratio L_0/L occurs for short fins compared to uninsulated fin tip.

For long fins these differences vanish.

Nomenclature

Bi	Biot number (hp/k_w)
c_p	specific heat at constant pressure
D	mass diffusivity
e	wall thickness
E	e / p
h	heat transfer coefficient
h_{fg}	latent heat of condensation
k	thermal conductivity
K	k_f / k_w
K_m	mass transfer coefficient ($kg/s{\cdot}m^2$)
l	fin length
l_0	length of the wet part of the pin
L	l/p
Le	Lewis number (α / D)
p	half-fin pitch
P	t/p
t	half-tin thickness
T	temperature
W	humidity ratio
x	coordinate ratio
X	x / p

Greek symbols

α thermal diffusivity
δ convergence factor
ε effectiveness of the fin assembly
θ dimensionless temperature $[(T - T_2) / (T1 - T_2)]$
ϕ relative humidity

Subscripts

b fin base
d dew point
f fin
t tip
w wall
0 at l_0
1 cold fluid
2 moist air

Superscript
* unfinned

References

[1] **Threlkeld, J.L.,** *Thermal Environmental Engineering,* Ch. 12, Prentice-Hall, Inc.k (1970).

[2] **McQuiston, F.C.,** Fin efficiency with combined heat and mass transfer, *ASHRAE Transactions.* **81**(1): 350-355 (1975).

[3] **Coney, J.E.R., Kazeminejad, H.** and **Sheppard, C.G.W.,** Dehumidification of air on a vertical rectangular fin: a numerical study. *Proc. Instn. Mech. Engrs, Part C,* **203:** 165-175 (1989).

[4] **Coney, J.E.R., Kazeminejad, H.** and **Sheppard, C.G.W.,** Dehumidification of turbulent air flow over a thick fin: an experimental study. *Proc. Instn. Mech. Engrs., Part C,* **203:** 177-188 (1989).

[5] **Sarma, P.K., Chary, S.P.** and **Dharma, Rao, V.,** Condensation on a vertical plate fin of variable thickness. *Int. J. Heat Mass Transfer,* **31:** 1941-1944 (1988).

[6] **Kazeminejad, H., Yaghoubi, M.A.** and **Bahri, F.,** Conjugate forced convection-conduction analysis of the performance of a cooling and dehumidifying vertical rectangular fin. *Int. J. Heat Mass Transfer,* **36:** 3625-3631.

[7] **Han-Taw Chen, Zen Lan** and **Tzung-I Wang,** Study of conjugate conduction-laminar film condensation for a vertical plate fin. *Int. J. Heat Mass Transfer,* **37:** 2592-2597 (1994).

[8] **Wu, G.** and **Bong, T.Y.,** Overall efficiency of a straight fin with combined heat and mass transfer, *ASHRAE Transactions, Part 1,* pp. 367-374 (1994).

[9] **Kazeminejad, H.,** Analysis of one dimensional fin assembly heat transfer with dehumidification, *Int. J. Heat Mass Transfer,* **38:** 455-462.

[10] **ASHRAE Handbook Fundamentals, Ch. 5 & Ch. 5,** *American Society of Heating, Refrigerating and Air Conditioning Engineers, Inc.* (1989).

Appendix

A flow chart diagram for the performance analysis of partially-wet fin assembly.

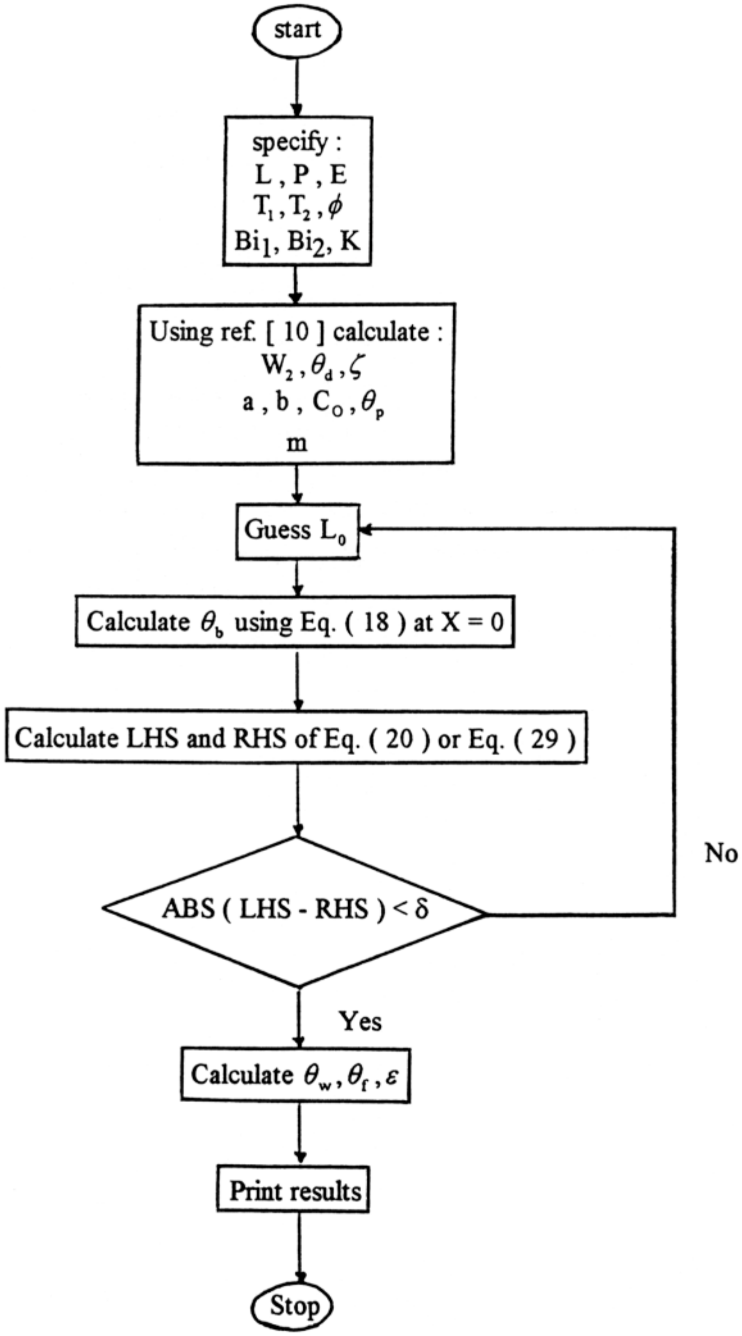

تحليـل أداء مجموعـة زعـانف مستطيـلة مبللـة جزئيًـا

مصطفى محمد صلاح الدين
** قسم الهندسة الميكانيكية ، كلية الهندسة والعمارة الإسلامية ، جامعة أم القرى*
مـــكة المكرمـــة - المملكة العربية السعودية

المستخلص . يقدم هذا البحث حلولاً تحليلية لأداء مجموعة زعانف مبللة كليًا أو جزئيًا . وقد تمت الحلول بفرض أن الرطوبة النسبية للهواء المشبع على السطح المبلل للزعانف تتغير خطيًا مع درجة حرارة الزعنفة عند هذا السطح .

ويحتوي البحث على دراسة تأثير العوامل المختلفة على أداء الزعانف وتوزيع درجات الحرارة بها . وتشمل هذه العوامل درجة حرارة المائع الباردة ودرجة حرارة الهواء والرطوبة النسبية له وكذلك معامل التوصيل الحراري للزعنفة وأبعاد مجموعة الزعانف إضافة إلى الشروط الحدية لطرف الزعنفة . علاوة على ذلك فإن النموذج المقدم في هذا البحث يفيد في تحديد الأجزاء المبللة والأجزاء الجافة من الزعانف .